Puay, How Tion; Hosoda, Takashi

Dam-Break Flow as a Means to Investigate the Flow Characteristics of Fluidable Material

DAM-BREAK FLOW AS A MEANS TO INVESTIGATE THE FLOW CHARACTERISTICS OF FLUIDABLE MATERIAL

How Tion Puay[1] and Takashi Hosoda[2]

[1] Phd Student, Department of Urban Management, Kyoto University
Kyodai Katsura, Nishikyo-ku, Kyoto, 615-8530, Japan, e-mail: puay.h@ht2.ecs.kyoto-u.ac.jp
[2] Professor, Department of Urban Management, Kyoto University
Kyodai Katsura, Nishikyo-ku, Kyoto, 615-8530, Japan, e-mail: hosoda@mbox.kudpc.kyoto-u.ac.jp

ABSTRACT

Dam-break flow has been an important problem in the study of shallow flow. In dam-break flow problem, water behind a gate is released by the instantaneous removal of the gate. In this study, instead of the commonly used dam-break flow with infinite extent, a more practical finite extent dam is used as a means to investigate the inertia- and viscous-flow regimes. Inviscid fluid is considered in the study of inertia-flow regime. In investigating viscous-flow regime, Newtonian and non-Newtonian fluids which represent the more common and simple viscous fluids, are considered. Theoretical studies of both inertia- and viscous-flow regimes are carried out and similarity solutions describing the regimes are derived. Theoretical findings are verified with two numerical models; a depth-averaged model (in the case of inviscid fluid only) and MPS (Moving Particle Semi-Implicit) Model.

Keywords: inertia-flow, viscous-flow and dam-break flow

1. INTRODUCTION

Dam-break flow has been intensively studied, analytically and experimentally, in the hydraulic engineering as a means to simulate actual dam-break failure and its effect such as surging waves and debris flow. The study of dam-break flow is also being used as a means to evaluate rheological properties. For example, Hosoda (1998) treated the slump flow test of fresh concrete as a problem similar to the phenomenon of dam-break flow of finite extent in his study of rheological properties of fresh concrete. Similarly, Shao and Lo (2003) also used the finite extent dam-break flow in the numerical simulations of some viscous fluids.

The existence of inertia- and viscous-flow regimes is clarified by Huppert (1982) in his study of viscous fluid flow over a horizontal channel. In this study, instead of the commonly used dam-break flow of infinite extent, a more practical finite-extent dam is used a means to investigate the inertia- and viscous-flow regimes.

This study is divided into 2 parts: the first part deals with the verification of inertia-flow regime by examining flow of inviscid fluid, while the second part investigates the viscous-flow regimes by using Newtonian and non-Newtonian fluids. In both parts, the propagation of wave front and the variation of depth at the origin are used as parameters to describe the flow characteristics.

2. INERTIA-FLOW REGIME

The flow from a sudden release of mass of inviscid fluid in a dam can be adequately described by the one-dimensional depth-averaged continuity and momentum equations:

$$\frac{\partial h}{\partial t}+\frac{\partial (hV)}{\partial x}=0 \tag{1}$$

$$\frac{\partial (hV)}{\partial t}+\frac{\partial (hV^2)}{\partial x}+gh\frac{\partial h}{\partial x}=0 \tag{2}$$

The parameters are described schematically in Figure 1 with h as depth of flow, V as flow velocity and g as the gravitational acceleration. The dam is located at $x=L_o$ with $x=0$ being the upstream boundary of the reservoir. The initial depth of the dam is set as h_o. At the upstream boundary, $q=hV=0$ or equivalently, $V=0$.

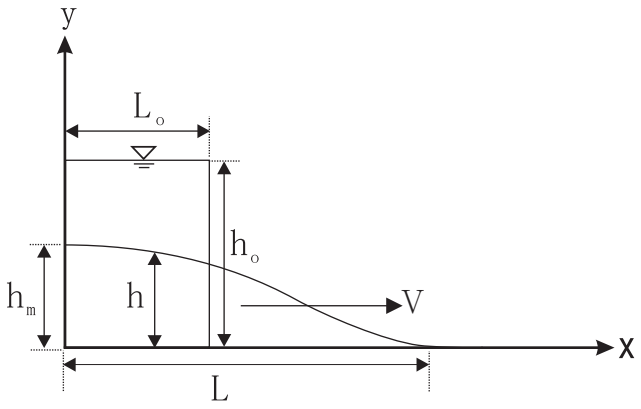

Figure 1. Dam-break flow of finite extent.

2.1 Depth near the origin of dam-break flow of finite extent

h and V are assumed to be expressible as a power series in x near $x=0$.

$$h(x,t)=h_m(t)+a_1(t)\left(\frac{x}{h_o}\right)+a_2(t)\left(\frac{x}{h_o}\right)^2+a_3(t)\left(\frac{x}{h_o}\right)^3+a_4(t)\left(\frac{x}{h_o}\right)^4+..... \tag{3}$$

$$V(x,t)=\sqrt{gh_o}\left[b_1(t)\left(\frac{x}{h_o}\right)+b_2(t)\left(\frac{x}{h_o}\right)^2+b_3(t)\left(\frac{x}{h_o}\right)^3+b_4(t)\left(\frac{x}{h_o}\right)^4+.....\right] \tag{4}$$

where $h_m(t)$ = time varying depth at $x=0$, $a_i(t)$ and $b_i(t)$ are functions of t to be determined and other parameters are defined as in Figure 1. Substituting Eq. 3 and Eq. 4 into Eq. 1 and grouping terms of the same order in x yields,

$$0^{\text{th}} \text{ order: } \frac{dh_m}{dt}+\sqrt{gh_o}\frac{h_m b_1}{h_o}=0 \tag{5}$$

$$1^{\text{st}}, 2^{\text{nd}}, 3^{\text{rd}} \text{ order in general form: } \frac{1}{h_o{}^n}\frac{da_n}{dt}+\frac{\sqrt{gh_o}}{h_o{}^{n+1}}\left[(n+1)h_m b_{n+1}+\sum_{j=1}^{n}(n+1)a_j b_{n-j+1}\right]=0 \tag{6}$$

where $n=$ 1, 2 and 3 for 1st, 2nd, and 3rd order respectively. Since V is expanded up to the order of 4 in the Taylor's series, the term $(n+1)h_m b_{n+1}$ is neglected in the case of 4th order. Similarly substituting Eq. 3 and Eq. 4 into Eq. 2 results in:

$$0^{\text{th}}\text{ order: } \frac{gh_m{}^2 a_1}{h_o} = 0 \tag{7}$$

$$1^{\text{st}}\text{ order: } \frac{\sqrt{gh_o}}{h_o}\frac{d}{dt}(h_m b_1) + \frac{g}{h_o}\left(2h_m b_1{}^2\right) + \frac{g}{h_o{}^2}\left(2h_m a_2 + a_1{}^2\right) = 0 \tag{8}$$

$$2^{\text{nd}}\text{ order: } \frac{\sqrt{gh_o}}{h_o{}^2}\frac{d}{dt}(h_m b_2 + a_1 b_1) + \frac{g}{h_o{}^2}\left(6h_m b_1 b_2 + 3a_1 b_1{}^2\right) + \frac{g}{h_o{}^3}(3h_m a_3 + 3a_1 a_2) = 0 \tag{9}$$

$$3^{\text{rd}}\text{ order: } \frac{\sqrt{gh_o}}{h_o{}^3}\frac{d}{dt}(h_m b_3 + a_1 b_2 + a_2 b_1) + \frac{g}{h_o{}^3}\left[4h_m\left(b_2{}^2 + 2b_1 b_3\right) + 8a_1 b_1 b_2 + 4a_2 b_1{}^2\right]$$
$$+ \frac{g}{h_o{}^4}\left[4h_m a_4 + 4a_1 a_3 + 2a_2{}^2\right] = 0 \tag{10}$$

From Eq. 7, $a_1 = 0$ and therefore from Eq. 6, with $n = 1$, $b_2 = 0$. Consequently, from Eq. 9 and Eq. 6 with $n = 3$, $a_3 = 0$ and $b_4 = 0$. By defining dimensionless variables, $t' = t\sqrt{gh_o}/h_o$, $h'_m = h_m/h_o$, $a'_2 = a_2/h_o$, $a'_4 = a_4/h_o$, we obtain the dimensionless equations as follows:

Continuity equation:

$$0^{\text{th}}\text{ order: } \frac{dh'_m}{dt'} + h'_m b_1 = 0 \tag{11}$$

$$2^{\text{nd}}\text{ order: } \frac{da'_2}{dt'} + 3h'_m b_3 + 3a'_2 b_1 = 0 \tag{12}$$

$$4^{\text{th}}\text{ order: } \frac{da'_4}{dt'} + 5a'_2 b_3 + 5a'_4 b_1 = 0 \tag{13}$$

Momentum equation:

$$1^{\text{st}}\text{ order: } \frac{d}{dt'}(h'_m b_1) + 2h'_m b_1{}^2 + 2h'_m a'_2 = 0 \tag{14}$$

$$3^{\text{rd}}\text{ order: } \frac{d}{dt'}(h'_m b_3 + a'_2 b_1) + 8h'_m b_1 b_3 + 4a'_2 b_1{}^2 + 4h'_m a'_4 + 2a'_2{}^2 = 0 \tag{15}$$

Power-law solutions of the form: $h'_m = \hat{A}t'^a, a'_2 = \hat{B}t'^b, a'_4 = \hat{C}t'^c, b_1 = \hat{D}t'^d, b_3 = \hat{E}t'^e$ are found where, $d = -1, b = -2, a + e = -3$ and $a + c = -4$ leading to:

$$\hat{D} = -a,\ \hat{A}\hat{E} = \frac{1}{3}(2 + 3a)\hat{B},\ 5\hat{B}\hat{E} = (6a + 4)\hat{C},$$
$$\hat{B} = -\frac{1}{2}a(a + 1),\ \hat{A}\hat{C} = -\frac{1}{2}\hat{B}^2 + \frac{1}{6}\hat{B}\left(6a^2 + 8a + 3\right) \tag{16}$$

From Eq. 16, the following equation for a can be derived:

$$a(a + 1)(3a + 2)\left(10a^2 + 12a + 3\right) = 0 \tag{17}$$

with solutions $a = -1$, $a = -2/3$, $a = -\left(6 \pm \sqrt{6}\right)/10$ and $a \neq 0$. Therefore, the possible temporal variation of the depth at the origin h_m can be expressed as follows:

$$a=-1,\quad \hat{B}=0,\ h'_m=\hat{A}t'^{-1}\ \rightarrow\ \ h_m\propto t^{-1} \tag{18}$$

$$a=-\frac{2}{3},\ \hat{B}=\frac{1}{9},\ h'_m=\hat{A}t'^{-\frac{2}{3}}\rightarrow h_m\propto t^{-\frac{2}{3}} \tag{19}$$

$$a=-\frac{1}{10}\left(6\pm\sqrt{6}\right),\ \hat{B}=\frac{1}{100}\left(9\pm\sqrt{6}\right),\ h'_m=\hat{A}t'^{-\frac{1}{10}\left(6\pm\sqrt{6}\right)}\rightarrow h_m\propto t^{-\frac{1}{10}\left(6\pm\sqrt{6}\right)} \tag{20}$$

In the case of $a=-2/3$ or $a=-\left(6\pm\sqrt{6}\right)/10$, the positive value of $\hat{B}$ implies a concave free-surface profile near the origin, which is unlikely to occur in the instantaneous release of fluid volume from the dam. For $a=-1,\ \hat{B}=\hat{C}=0$ and the profile near the origin $h(x,t)=\hat{A}t'^{-1}h_o$ implies a horizontal free-surface near the origin. Therefore $a=-1$ is chosen as the appropriate solution. This power-law solution is only valid for $t>L_o/c_o$ as the depth at the origin begins to decrease immediately after $t=L_o/c_o$ where c_o is the celerity of the flow.

2.2 Wave front position of dam-break flow of finite extent

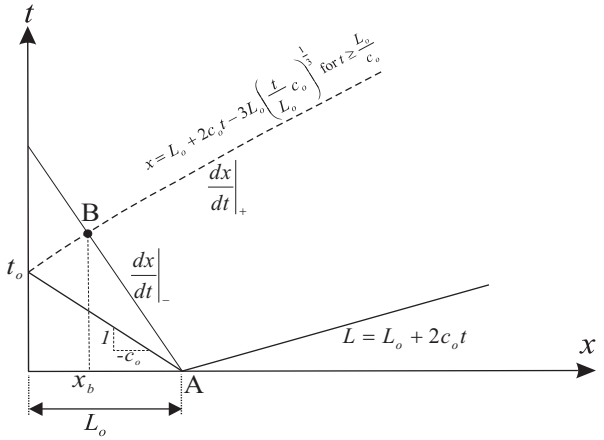

Figure 2. Characteristic lines of dam-break flow of finite extent

By solving the governing depth-averaged equation of motion using the method of characteristics (MOC), the analytical solution for temporal variation of the wave front, L due to the release of fluid behind an infinite-extent dam can be obtained, (Jain, 2001) and the solution is given by

$$L=L_o+2\sqrt{gh_o}t\rightarrow L\propto t \tag{21}$$

In the case of finite-extent dam-break flow, the position of the first negative wave reflected by the upstream wall (represented by dotted line in Figure 2) can be determined by solving for position at point B, x_b in Figure 2 using characteristic lines, (Hogg, 2006).

$$x_b=L_o+2c_ot-3L_o\left(\frac{c_ot}{L_o}\right)^{\frac{1}{3}} \tag{22}$$

Comparing Eq. 21 and Eq. 22 reveals that the negative wave reflected by the upstream wall

always trails behind the front propagation wave, and therefore will not affect the flow in the region between the wave front and the disturbance. Therefore Eq. 21 is valid for dam-break flow of finite extent as well.

3. VISCOUS-FLOW REGIME

3.1 Theoretical Analysis

The momentum equations for viscous fluid can be written as in Eq. 23.

$$\frac{D\tilde{V}}{Dt} = -\frac{\nabla P}{\rho} + \tilde{g} + \frac{1}{\rho}\nabla \cdot \tau \tag{23}$$

In the x direction, for 2-dimensional case, Eq. 23 can be written as follows:

$$\frac{\partial u}{\partial t} + u\frac{\partial u}{\partial x} + v\frac{\partial u}{\partial y} = -\frac{1}{\rho}\frac{\partial P}{\partial x} + g_x + \frac{1}{\rho}\frac{\partial \tau_{yx}}{\partial y} \tag{24}$$

By assuming that the flow is slow, the inertia term on the left hand side of Eq. 24 can be neglected compared to the pressure and stress term. Therefore, in the case of horizontal flow where $g_x = 0$, we could equate the pressure term and stress term. By assuming static pressure distribution, shear stress τ_{yx} over the depth of flow, h can be written as follows:

$$\tau_{yx} = \int \frac{\partial P}{\partial x}\, dy = -\rho g \frac{dh}{dx}(y - h) \tag{25}$$

Power-Law model is used to define the shear stress- rate of strain relations for general viscous fluid here, and is written in its general form as in Eq. 26 with $K =$ viscosity coefficient and $n =$ flow index. For Newtonian fluid, $n = 1$, while for non-Newtonian fluid; $0 < n < 1$ in the case of shear-thinning fluid and $n > 1$ in the case of shear-thickening fluid.

$$\tau = K\left(\frac{\partial u}{\partial y}\right)^n \tag{26}$$

By substituting Eq. 26 into Eq. 25, velocity distribution can be derived as follows:

$$u = \frac{n}{n+1}\left[\frac{\rho g}{K}\frac{dh}{dx}\right]^{\frac{1}{n}} h^{1+\frac{1}{n}}\left[1 - \left(1 - \frac{y}{h}\right)^{1+\frac{1}{n}}\right] \tag{27}$$

Therefore, the depth-averaged velocity in x direction, $\overline{U}$ can be derived as well.

$$\overline{U} = \frac{1}{h}\int_0^h u\, dy = \frac{n}{2n+1}\left[\frac{\rho g}{K}\frac{dh}{dx}\right]^{\frac{1}{n}} (h)^{1+\frac{1}{n}} \tag{28}$$

This velocity distribution also agrees with the velocity distribution of viscous fluid flowing down an inclined plane by Ng and Mei (Ng and Mei, 1994). By using Eq. 25 and Eq. 28, an expression describing the relation between bottom shear stress, τ_b and depth-averaged velocity, $\overline{U}$ can be derived as follows:

$$\tau_b = K\left(\frac{2n+1}{n}\right)^n\left(\frac{\overline{U}}{h}\right)^n \tag{29}$$

The relation in Eq. 29 also agrees with the derivation made by Ng and Mei (Ng and Mei, 1994) for viscous flow down an inclined plane. The velocity distribution and bottom shear stress derived in Eq. 27 and Eq. 29 satisfy zero velocity at bottom boundary and vanishing shear stress at free surface. Therefore, for general viscous fluid, the depth-averaged equation of motion of can be written as follows:

$$\frac{\partial h}{\partial t} + \frac{\partial}{\partial x}\left(\overline{U}h\right) = 0 \tag{30}$$

$$\frac{\partial}{\partial t}\left(h\overline{U}\right) + \frac{\partial}{\partial x}\left(\hat{\beta}h\overline{U}^2\right) + gh\frac{\partial h}{\partial x} = -\frac{\tau_b}{\rho} = -\frac{K}{\rho}\left(\frac{2n+1}{n}\right)^n\left(\frac{\overline{U}}{h}\right)^n \tag{31}$$

Similarity functions $p(\xi)$ and $q(\xi)$ are introduced for the depth and velocity of flow as follows:

$$h = h_m(t)p(\xi) \tag{32}$$

$$V = V_m(t)p(\xi) \tag{33}$$

$$\xi = \frac{x}{L(t)} \tag{34}$$

$L(t)$ is the wave front position measured from the origin as shown in Figure 1. The boundary conditions for the similarity functions of $p(\xi)$ and $q(\xi)$ are:

$$p(0) = 1,\ p(1) = 0,\ q(0) = 0 \tag{35}$$

By assuming similarity solutions exist for h_m, V_m and L_m:

$$h_m = \alpha h_o\left(\sqrt{\frac{g}{h_o}}t\right)^a, V_m = \beta\sqrt{gh_o}\left(\sqrt{\frac{g}{h_o}}t\right)^b,\ L = \gamma L_o\left(\sqrt{\frac{g}{h_o}}t\right)^c \tag{36}$$

where h_o is the characteristic depth and L_o is the characteristic length. The dimensionless form for time t' is introduced as follows:

$$t' = \sqrt{\frac{g}{h_o}}t \tag{37}$$

By utilizing Eq. 36, the expression of depth and velocity of flow in similarity solutions form are substituted into the governing equation in Eq. 23 and Eq. 24. Therefore, the governing equations can be written in dimensionless form of time, t' as follows:

Continuity Equation:

$$\alpha h_o a t'^{a-1}\sqrt{\frac{g}{h_o}}p(\xi)-\alpha h_o a c t'^{a-1}\xi\sqrt{\frac{g}{h_o}}\frac{dp(\xi)}{d\xi}$$
$$+\frac{\alpha\beta}{\gamma L_o}h_o\sqrt{gh_o}q(\xi)\frac{dp(\xi)}{d\xi}t'^{a+b-c}+\frac{\alpha\beta}{\gamma L_o}h_o\sqrt{gh_o}p(\xi)\frac{dq(\xi)}{d\xi}t'^{a+b-c}=0 \tag{38}$$

Momentum Equation:

$$\alpha\beta b g h_o p(\xi)q(\xi)t'^{a+b-1}-\alpha\beta c g h_o\xi\, p(\xi)\frac{dq(\xi)}{d\xi}t'^{a+b-1}+\alpha\beta a g h_o p(\xi)q(\xi)t'^{a+b-1}$$
$$-\alpha\beta c g h_o\xi q(\xi)\frac{dp(\xi)}{d\xi}t'^{a+b-1}+\hat{\beta}\frac{\alpha\beta^2}{\gamma}\frac{gh_o^{\,2}}{L_o}q^2(\xi)\frac{dp(\xi)}{d\xi}t'^{a+2b-c}$$
$$+2\hat{\beta}\frac{\alpha\beta^2}{\gamma}\frac{gh_o^{\,2}}{L_o}p(\xi)q(\xi)\frac{dq(\xi)}{d\xi}t'^{a+2b-c}+\frac{\alpha^2}{\gamma}\frac{gh_o^{\,2}}{L_o}p(\xi)\frac{dq(\xi)}{d\xi}t'^{2a-c}$$
$$=\frac{K}{\rho}\left(\frac{2n+1}{n}\right)^n\left(\frac{\beta}{\alpha}\sqrt{\frac{g}{h_o}}\frac{p(\xi)}{q(\xi)}t'^{b-a}\right)^n \tag{39}$$

By equating the power of t' in the continuity equation in Eq. 38, the following relations of coefficients is obtained:

$$b-c=-1 \tag{40}$$

For constant volume of flow

$$V=h_m L\int_0^1 p(\xi)\,d\xi=\alpha\gamma h_o L_o\left(\sqrt{\frac{g}{h_o}}t\right)^{a+c}\int_0^1 p(\xi)\,d\xi\rightarrow\ \therefore a+c=0 \tag{41}$$

It is assumed that in the case of viscous-flow regime, the flow is governed by the dynamic equilibrium of pressure and viscosity. Therefore, by equating the power of t' between pressure and viscous terms in Eq. 39, we can write the following relations between the coefficients,

$$2a-c=n(b-a) \tag{42}$$

By solving Eq. 40, Eq. 41 and Eq. 42;

$$a=-\frac{n}{3+2n},\qquad c=\frac{n}{3+2n} \tag{43}$$

Thus, the temporal variation of the depth at the origin, h_m and wave front propagation, L can be written as follow:

$$h_m = \alpha h_o \left(\sqrt{\frac{g}{h_o}} t \right)^a \quad \rightarrow \quad h_m \propto t^{-\frac{n}{3+2n}} \tag{44}$$

$$L = \gamma L_o \left(\sqrt{\frac{g}{h_o}} t \right)^c \quad \rightarrow \quad L \propto t^{\frac{n}{3+2n}} \tag{45}$$

4. NUMERICAL SIMULATION AND RESULTS

4.1 Numerical Simulation Models

Two models are used to verify the analytical results: a depth-averaged model with Harten (1983)'s TVD (Total Variation Diminishing) scheme and a particle-based model, MPS (Moving Particle Semi-Implicit) which is originally used to solve the governing Navier-Stokes equation of motion (Koshizuka and Oka, 1996). MPS is used as an alternative numerical simulation model as setup is fairly easy due to its grid-less nature and its ability to handle complicated free surface flow (Gotoh et al., 2005). Although the MPS approach does not directly solve the governing depth-averaged equations used in the analytical analysis, the solution of Navier-Stokes equation by the MPS model can be approximated by the solution of depth-averaged model.

4.2 Results

Simulations of inviscid fluid are carried out with depth-averaged model with Harten's TVD scheme and MPS model, while the simulations of viscous fluid are carried out using MPS model only. Simulations conditions are shown in Table 1. During the simulations, wave front propagation and temporal variation of depth at the origin are observed. The results for the case of inviscid fluid are shown in Figure 3, while for the case of Newtonian and non-Newtonian fluids (shear thickening and shear thinning), the results of simulation are shown in Figure 4, Figure 5 and Figure 6 respectively.

Table 1 Temporal variation of wave front and depth of flow at the origin, and numerical simulation conditions.

Fluid type	Flow index n	Wave front $L \propto t^{\frac{n}{3+2n}}$	Depth at origin $h_m \propto t^{-\frac{n}{3+2n}}$	Numerical simulation condition Initial dam size: h_o=0.5m, L_o=0.5m
Inviscid	-	$L \propto t$	$h_m \propto t^{-1}$	-
Newtonian	1	$L \propto t^{\frac{1}{5}}$	$h_m \propto t^{-\frac{1}{5}}$	Kinematic viscosity, ν 1) ν=0.0005Pa.s
Non-newtonian Shear thickening	2	$L \propto t^{\frac{2}{7}}$	$h_m \propto t^{-\frac{2}{7}}$	Consistency, K 1) K=0.01 Pa.s^2 2) K=1.0 Pa.s^2
Shear thinning	1/2	$L \propto t^{\frac{1}{8}}$	$h_m \propto t^{-\frac{1}{8}}$	1) K=0.01 Pa.s$^{1/2}$ 2) K=1.0 Pa.s$^{1/2}$

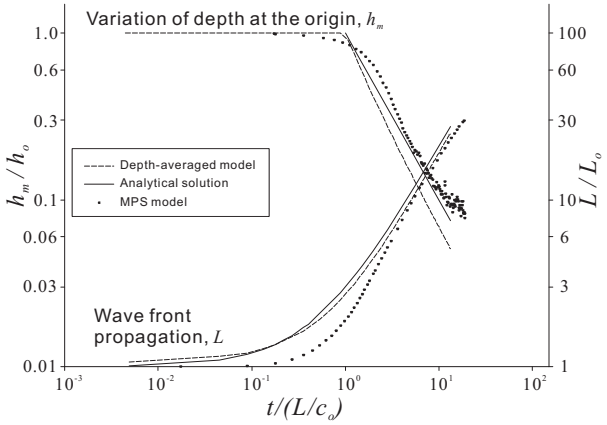

Figure. 3 Temporal variation of depth at the origin, h_m and wave front, L propagation for inviscid fluid

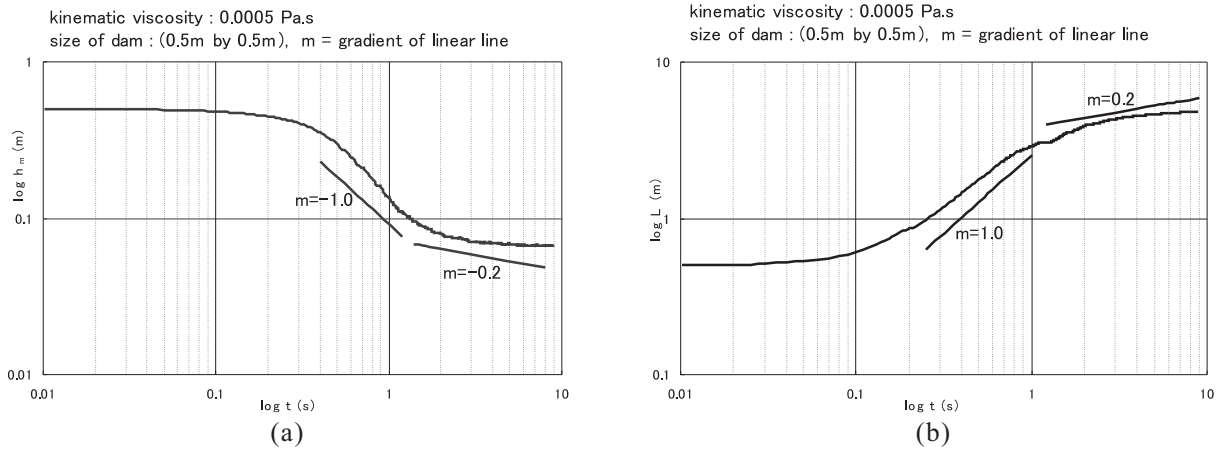

Figure 4. Temporal variation of a) depth at the origin, h_m and b) wave front, L for Newtonian fluid.

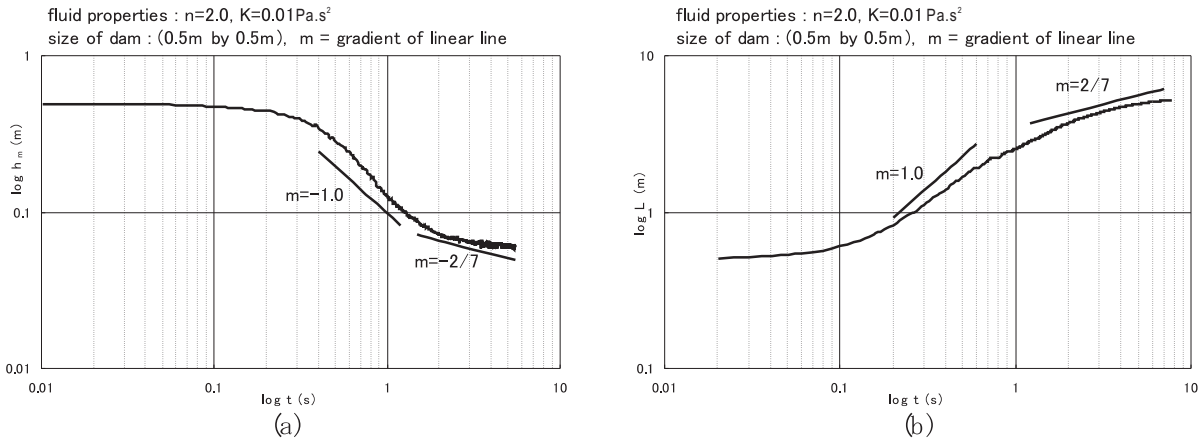

Figure 5. Temporal variation of a) depth at the origin, h_m and b) wave front, L for non-Newtonian fluid of shear thickening type.

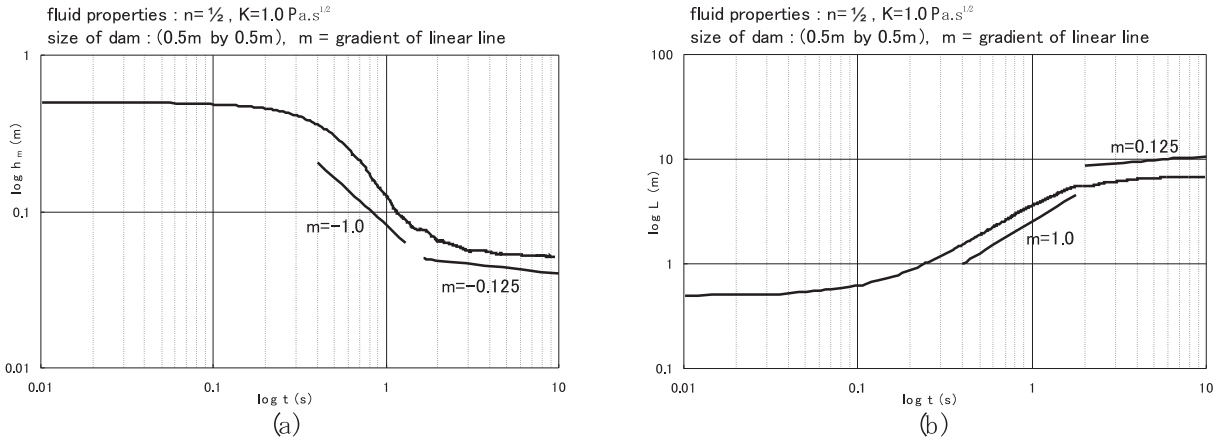

Figure 6. Temporal variation of a) depth at the origin, h_m and b) wave front, L for non-Newtonian fluid of shear thinning type.

5. CONCLUSION

Inertia- and viscous-flow regimes are investigated in this study by examining inviscid and viscous fluids independently. The temporal variation of the flow depth at the origin, h_m and wave front, L propagation are used as parameters to describe the characteristics of the regimes. Analytical results for both inertia- and viscous-flow regimes show satisfactory agreement with numerical simulation results. It is envisaged that the simple mathematical methods used here could be improved for wider applicability. In the sense of engineering applications, the findings of characteristics regimes can be used to verify experimental or numerical simulation results of simple viscous fluid.

REFERENCES

Gotoh, H., Ikari, H., Memita, T. and Sakai, T. (2005), Lagrangian particle method for simulation of wave overtopping on a vertical seawall, *Coastal Eng. J.*, Vol. 47, Nos 2 & 3, pp.157-181.

Hogg, A. J. and Pritchard, D. (2004), The effect of hydraulics resistance on dam-break and other shallow inertial flows, *J. Fluid Mech.,* Vol. 501, pp.179-212.

Hosoda, T., Kokada, T. and Miyagawa, T. (1998), Study on a method of obtaining yield values of fresh concrete from slump flow test, *Concrete Lib. Of JSCE*, Vol. 32, pp.29-41.

Huppert, H.E. (1982), The propagation of two dimensional and axisymmetric viscous gravity currents over a rigid horizontal surface, *J. Fluid. Mech.*, Vol. 121, pp.43-58.

Jain, S.C. (2001), Open Channel Flow, John Wiley and Sons, Inc., New York.

Koshizuka, S., Nobe, A. and Oka, Y. (1998), Numerical analysis of breaking waves using the moving particle semi-implicit method, *Int. J. Num. Meth. Fluids*, Vol. 26, pp.751-769.

Shao, S. and Edmond Lo, Y.M. (2003), Incompressible SPH and method for simulating Newtonian and non-Newtonian flows with a free surface, *Adv. in Water Resource*, Vol. 26(7), pp.787-800(14).

Ng, C. and Mei, C.C. (1994), Roll waves on shallow layer of mud modelled as a power-law fluid, *J. Fluid Mech.*, Vol. 263, pp.151-183.